

## Cellular Beams with Closely Spaced Web Openings – A Review of Analytical Calculation Models for Web-Post Buckling

Przemysław Saternus<sup>1</sup>

<sup>1</sup> Kielce University of Technology, Faculty of Civil Engineering and Architecture, Al. Tysiąclecia Państwa Polskiego 7, 25-314 Kielce, Poland  
e-mail: psaternus@tu.kielce.pl

### ABSTRACT

This paper is devoted to cellular beams manufactured by flame cutting and welding of hot rolled I-sections. The influence of fabrication processes on the size of geometric and material imperfections was considered. Static performance was characterised, as were the failure modes, with particular emphasis on the Vierendeel mechanism and web-post buckling. As the literature review shows, a local loss of web post stability is a frequent failure mode of cellular beam with closely spaced web openings. The main objective of this paper is present a summary of research on web post buckling (WPB) in cellular beams in light of the available analytical computational methods for determining WPB resistance based on the analogy to compression member buckling. This paper addresses the need for a clear assessment of the discrepancies between the assumptions and calculation algorithms used in the presented methods, so far lacking in the literature. This paper includes an explanation of the essence of the WPB phenomenon, a summary of the basic assumptions and algorithms used in the available methods, a description of the differences between them, and a critical comparison of these methods. The presented algorithms were unified and adjusted to the nomenclature of PN-EN 1993-1-1. For 7 cellular beams, the analytical column buckling resistance under the action of vertical shear force was determined according to 5 analytical methods implemented in MS Excel. The results were presented in tabular and graphical forms. Significant discrepancies between the results from the different methods were shown and discussed. The assumptions of the methods vary significantly. The largest differences between the predicted resistances were observed for narrow posts, while for wider posts, the methods showed better agreement. The lack of clear consensus on the correct design procedure does not encourage designers to optimally design such load-bearing members or may lead to construction disasters. This article indicates the points of disagreement concerning the calculation models used and outlines the direction for further work. A step for future work will be to verify the assumptions of numerical models and establish clear guidelines for designers in the field of analytical calculations.

**Keywords:** cellular beams, perforated steel beams, web-post buckling, vertical shear capacity, strut model, analytical methods.

### INTRODUCTION

Currently, cellular beams are being used more often in modern buildings and industrial structures. The static behaviour theory and mechanisms of cellular beams failure refer to the so-called Vierendeel girder developed as a new type of metal bridge girder at the end of the 19th century by a Belgian engineer, Professor Arthur Vierendeel [1]. The theory of designing perforated beams welded from hot-rolled I-sections

or C-sections that emerged in the second half of the 20th century was based on the concept of the Vierendeel bridge girder. A perforated beam is fabricated, for example, by cutting an I-section along a broken line around the centre line of the web, repositioning the resulting T-sections and re-welding the two halves in the place of the so-called posts. The web openings can be rectangular, round, oval, hexagonal, or another shape resulting from the cutting method [2]. A post is understood to be a solid web area between the

openings. The idea behind this solution is to obtain a section that is about 30–60% deeper than the parent section. Thus, its bending stiffness increases about the stronger axis without increasing the amount of steel used.

Furthermore, the openings located between the T-sections of a cellular beam can be used to pass the service within the depth of the section. First such load-bearing elements were produced in the USA, then in Argentina (the 1930s), Japan, the UK and Germany at the beginning of the 20th century. However, due to the high cost of production, they did not gain popularity in less prosperous countries. It was only since the 1980s, with the evolution of cutting and welding processes, that beams with sequential web openings were re-examined on a larger scale, gaining more popularity in the 1990s with the development of automated cutting. Today, cellular beams find many applications, such as floor beams, hall portal frames, purlins, columns, and beams in composite floors.

Large, sequentially placed openings in the web enable flexible service distribution. Larger cross-sections of service ducts accommodate building services and integrate them with the structural elements without reducing the room area. In addition, increased stiffness of perforated beams enables constructing large spans without adding weight, such as car parks, roofs and ceilings of commercial and service facilities, sports and recreation or industrial facilities (e.g., shipyards), footbridges. The openwork structure gives the impression of lightness and ensures high aesthetics.

Automation of steel beam production processes eliminated manual cutting and welding costs, making the prefabrication of a new beam generation profitable again. The shapes of the openings have been optimised, and their complex geometry is an additional architectural value [3]. Initial geometric imperfections of ready-made perforated steel elements also decreased. One of the lead manufacturers claims that for beams with circular openings and cross-section depths not exceeding 600 mm, the maximum horizontal out-of-plane deviation of the beam web does not exceed 4 mm; the tolerance of the perforated section depth is +3/-5 mm; the misalignment of tees with respect to the vertical axis at the weld is up to 2 mm; the opening diameter tolerance is +5/-2 mm; the longitudinal shift of the upper and lower tees is less than 0.03% of the total beam length [4]. Account should also be taken of the presence of

geometric imperfections in the original solid wall elements, such as deviations due to the allowable tolerances for wall thickness, width and height, as well as the radius of curvature. The same applies to material imperfections. Residual stresses in the original member that occurred as a thermal effect of the hot rolling process are adversely increased by residual stresses from the perforated beam manufacture processes [5]. A beam with circular openings is produced by making double cut-outs along the entire length of the element. This process results in a continuous series of semi-circles and straight sections parallel to the horizontal axis of the element. Profiling is a fully computerised thermal process of oxygen or plasma torch cutting. In the next step, the separated tees are repositioned and re-joined into a perforated I-section by butt welding with, for example, the MAG welder. These stages cause uneven heat exposure that facilitates the development of additional internal stresses. Internal stresses in cellular beams are higher than in the beams with hexagonal openings due to the greater intensity of thermal processes used for making double cut-outs in the web. Internal residual stresses combined with uniform external stresses lead to premature non-linear, non-elastic behaviours of the web material before the stress from external loads reaches the yield strength of the material. This is because the residual stresses add up with the principal longitudinal stresses acting in the same direction. The effect of the manufacturing process on the increase of residual stresses (the maximum residual compressive stresses in particular) in a perforated component reduces the buckling strength by about one buckling curve [6]. The buckling curve “c” from EC3 [7] gives generally satisfactory results for the geometry of most of the perforated sections used. Sonck and Belis [6] numerically and experimentally investigated the buckling curve fit for elastic lateral-torsional buckling and showed that using the buckling curve “c” provides small dangerous displacements for the parent section HE320A and substantial safe displacements for HE320M. By adopting the c buckling curve, it is possible to safely take account of the effect of geometric imperfections and residual stresses on the buckling behaviour of the member.

In the classical calculation model for a cellular beam (secured against spatial loss of stability), the limit state strength of chords and posts is determined based on the interaction of longitudinal force, bending moment and transverse force

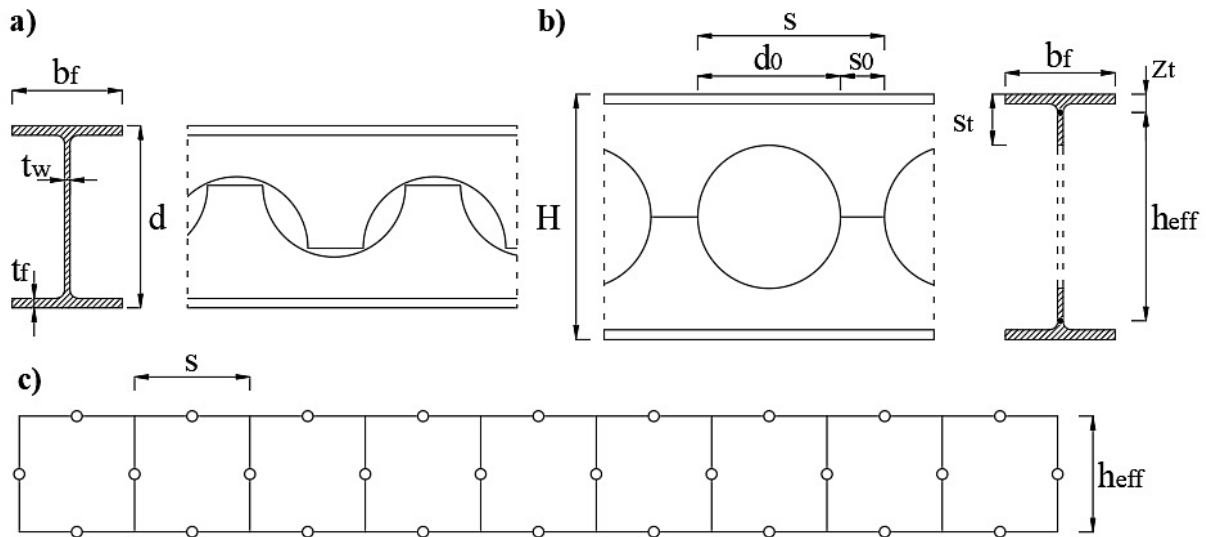


Fig. 1. Basic designations for: a) the parent section, b) the perforated section, c) the static scheme

[8, 9]. The calculation scheme is a frame with rigid nodes in which flanges are represented by horizontal bars, whereas posts are represented by vertical bars. Horizontal bars run in the centroid of the flanges with a depth of  $s_p$ , at a distance  $z_t$  from the extreme fibres, Figure 1. Vertical bars with a length of  $h_{eff}$  cross the centre of symmetry of the post to connect with the horizontal bars in the nodes. This system is  $3n$  times hyperstatic, where “ $n$ ” represents the number of segments in the beam. A single segment is an area between the vertical axes of the posts; thus, its length  $s$  corresponds to the sum of the opening diameter  $d_o$  and the width of the post  $s_o$  (Fig. 1). The simplified calculation scheme introduces hinges in the middle of the lengths of the sections between the nodes of the horizontal and vertical bars in each beam segment. These are the intersection points of the bending moment diagram, where the bending moment is zero. Deflection occurs due to the bending moment and shear force. Their influence is much more significant than in the case of a beam without openings. The shear force causes secondary Vierendeel bending moments. The moment in a segment node is half the transverse design force in the middle section of the segment in question, acting on the lever arm equal to half the width of this segment. The interaction of secondary moments with global bending moments generates local axial forces in the flanges and mating web parts. Therefore, it is necessary to check the safety of the web post cross-sections, the upper and lower flange under the action of the longitudinal force, and bending moment and transverse force calculated under the Vierendeel beam

model. The interaction of compression, bending and shear may be neglected if the transverse force does not exceed 50% of the plastic shear capacity of the cross-section [7]. If this condition is not met, the effect of shear can be considered by assuming a reduced section design resistance and reduced yield stress in the active field shear.

The spacing of the chords increases the bending stiffness about the stronger axis  $y-y$  but does not improve the stiffness of the perforated section about the weaker axis  $z-z$ . Additionally, due to the web openings, the torsional stiffness of the perforated section is reduced (relative to a solid beam). Therefore, increased susceptibility is observed of the bending component to a spatial loss of stability such as lateral-torsional buckling (LTB), web distortional buckling (WDB), web-post buckling (WPB), Vierendeel mechanism (VM), or the interaction of several forms of instability [10, 11, 12, 13]. Design procedures considering various failure modes are available in the literature [14, 15].

The beam can transfer additional load until four plastic hinges develop at the ends of the tees near the opening corners, which is understood as the Vierendeel mechanism [16, 17]. The development of local yielding and the influence of the cut-out geometry on the VM have been the subject of many studies reported in the literature [18, 19].

In certain cases of technically important perforated web geometry, a different failure mechanism may occur - the web-post buckling between openings or, in some cases, the combined action of WPB and VM. For example, beams are particularly exposed to WPB when they are insensitive to lateral stability loss, and shear dominates

in the web. Then the load acting on the top chord generates shear stresses in the posts to transfer the tensile stresses to the bottom chord. As a result, a complex state of stress arises around the openings, leading to the post's buckling.

In the case of beams not protected against lateral loss of stability, web distortional buckling (WDB) combined with lateral-torsional buckling (LTB) may occur. During WDB, which is a local phenomenon, the web is bent over short distances without complete lateral deflection and twist. The phenomenon consists of the web's horizontal deformation with vertical deflection and the displacement of the nodes of the centreline of the compression flange. Usually, WDB and LTB occur together, resulting in a lateral distortional buckling (LDB) mechanism. In the classic LTB case, the web moves laterally and twists with the flanges as a rigid plate. The study of the interaction of these phenomena [11, 20] found that LTB becomes stronger with increasing slenderness of the beams, while WDB increases for short beams that are less prone to torsion.

The primary topic of this article is web-post buckling (WPB) in the light of available analytical calculation methods. Methods of load-bearing capacity assessment for WPB are presented against American specifications [21] and British standards [22] adjusted to the terminology and conditions of PN-EN 1993-1-1:2006 [7].

## VIERENDEEL BENDING (VM) AND WEB-POST BUCKLING (WPB)

The periodic presence of sections with different geometry and load capacity in the cellular beam causes many design problems even if the beam is secured against lateral-torsional buckling. Two typical failure mechanisms develop in this case: 1) a loss of load capacity due to the interaction of the axial force and additional bending of the chords, i.e., Vierendeel bending, and 2) web-post buckling. Tee compression and bending comprise the leading mechanism when the post is sufficiently wide and stiff (low susceptibility of the post to WPB) or when the openings are quite wide (elongated), and the web-flange tees are quite low (high susceptibility of the chords to VM). Due to the geometrical relationships of the cutting process in a solid-walled element to obtain round holes, the wide posts have a lower T-section cross-section. This is because cutting

along long straight lines (wider posts) requires an increased radius of the semi-circles (larger holes) that avoid them on the cutting path. For such a beam web geometry, when the external loads increase, plastic hinges propagate at the ends of the tee segments, i.e., around the corners of the openings. In this case, the beam resistance due to the flange yielding condition is generally lower than the shear buckling resistance of the post.

The WPB mechanism occurs first when the Vierendeel bending resistance of the chords is correspondingly greater than the shear resistance of a relatively narrow post. This is the case of closely spaced round holes when the tee sections above and below the openings are higher. The use of appropriately larger openings improves the global bending parameters but reduces the shear strength of the beam. It can be stated here that an optimally designed cellular beam is one in which the bending and shear resistances are similar. However, in this case, there may be a dangerous WPB and VM interaction manifested by a significant reduction in the load capacity of the designed beam [23]. In the case of a suitably narrow post, the interaction of WPB and VM consists of the development of yielding zones due to the second-order effects caused by the web-post buckling and their progress to the Vierendeel bending areas. The wider post is characterised by increased shear strength since the diagonal main (compressive) stresses propagate over a larger area. The failure mechanism can therefore be determined on the basis of geometrical relationships. Based on the experimental and numerical studies available in the literature [20, 28], it can be predicted that the beam will fail in the WPB mode if  $1.1 \leq s/d_o \leq 1.5$  and  $0.5 \leq d_o/H \leq 0.8$  and slenderness  $\lambda < 200$ , which covers the standard geometries of perforated beams.

Chung et al. [17] developed an algorithm for a critical failure mechanism of a perforated element under bending and shear moments based on the Vierendeel parameter and strength ratios. They also proposed formulas and empirical curves for the moment-shear interaction for establishing load-bearing capacities with different web openings. Generally, beams with rectangular or oval openings are more susceptible to Vierendeel bending than circular openings, where shear buckling behaviour in the web post is more important.

According to Hoffman et al. [24], in the simply supported beam with the uniformly loaded upper chord, the region with the highest risk of

failure is the web area between the edge of the first opening and the beam support node, and the area of the first post between the openings, where shear dominates. Łysa and Ruchwa [25] claim the ring-stiffening is the optimal solution for the web in the high shear zones to increase the stiffness to local stress concentrations around the openings. Local loss of web stability around various types of openings is now the leading research direction [26], particularly the beams secured against the lateral-torsional buckling. In her doctoral thesis, De Oliveira [27] established formulas for local buckling critical stresses in perforated beams using Rayleigh's energy method and validated them through MES numerical simulations. Tsavdaridis presented comprehensive analyses of stress field distribution in cellular beam posts in his doctoral thesis [28]. Similar studies were performed by Ward [29], Lawson et al. [15, 30], Bitar et al. [31], Tsavdaridis et al. [32, 33], Panedpojaman et al. [23], Wang et al. [34], and Grilo et al. [35]. As a result, analytical methods of WPB resistance estimation were developed based on similar observations but substantially differed in terms of developed algorithms. The literature lacks a reliable and critical comparison of all these methods contained in one document. Only some of the methods have been compared for limited design situations. The methods of Lawson [15, 30] and Panedpojaman [23] were compared by Zaher et al. [36], but only for cellular curved beams. Ferreira et al. [37] compared the methods of Lawson [15, 30], Panedpojaman [23] and Grilo [35], but only for composite cellular beams with a reinforced concrete slab. The methods were too conservative for composite beams and did not consider the beam-concrete slab cooperation or the influence of the end post width on the WPB resistance.

Research into the WPB and VM mechanisms is continued in order to build a reliable computational model. In 2021, Kang et al. [38] proposed a shear strength prediction model based on the DSM (Direct Strength Method). Furthermore, an analogy to the compression strut [15, 30, 32, 33, 23] is used to develop calculation methods for beams with hexagonal openings [39].

## OBJECTIVE OF THE STUDY

The primary objective of this study was to present a summary report on web post buckling (WPB) in cellular beams in light of available

analytical computational methods for determining the WPB resistance based on the analogy to buckling of compression members. As shown above, there is currently no study in the literature in which all these methods are presented in the way that makes an unambiguous assessment of the differences between the assumptions and calculation algorithms possible. There is a need to compile and compare what has been achieved to date on similar analytical methods in a single document. To make this possible, the design formulas of the different methods were adapted to the nomenclature used in EN 1993-1-1 [7] to finally determine the design resistance to the vertical shear force. The comparison will allow checking the degree of agreement between different methods and show possible reasons for deviations. This study is particularly important for designers of metal structures. Knowing the failure mechanisms and understanding the available design methods significantly increases awareness among designers. The lack of a clear consensus on the correct design procedure for determining the load carrying capacity for WPB discourages designers from designing optimal load-bearing members or may be the cause of structural failure.

## ANALYTICAL METHODS FOR THE ASSESSMENT OF VERTICAL SHEAR FORCE RESISTANCE DUE TO WPB

Beam webs with closely spaced openings are subject to vertical shear, which generates horizontal shear in the central part of the post. The horizontal shear force causes an internal secondary bending moment equal to zero in the mid-depth of the post. Its value increases towards the flanges according to the static scheme of the Vierendeel beam - the maximum value of the moment occurs in the node, Figure 2a. From the moment, normal stresses increase to the maximum value at the edges of the openings at a critical distance from the horizontal axis of the beam and then decrease, spreading over a larger area, Figure 2b. The horizontal shear force causes shear stresses inside the web that decrease towards the edge [35], Figure 2c. The maximum reduced stresses H-M-H are located at opening edges and the intersection point of post diagonals, Figure 2d.

The limiting vertical shear force in the upper tee is limited by the maximum Vierendeel bending resistance of the T-section (VM) and the shear

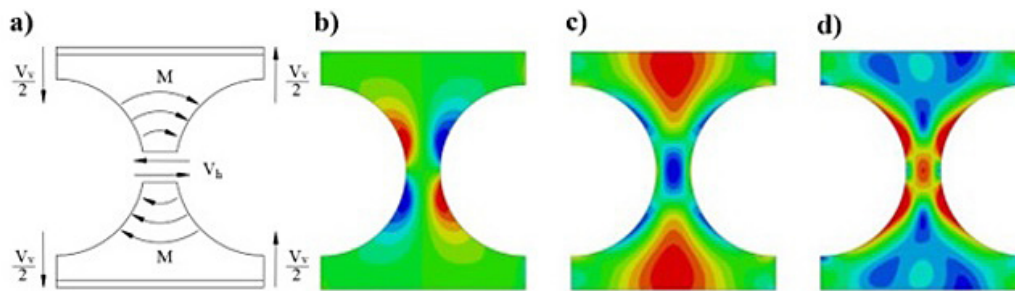


**Fig. 2.** Forces and stresses in the web post: a) force distribution, b) normal stresses, c) shear stresses, d) von Mises reduced stresses according to [35] (the red colour represents the highest positive values)

strength of web post-buckling (WPB). The plastic bending resistance is determined for class 1 of the T-section according to EC3 [7]. The web of a T-chord is treated as a cantilevered compression wall with a class 1 slenderness limit of  $9\epsilon$ ; otherwise, the load capacity should be determined based on the elastic properties of the cross-section. The critical section for the upper tee can be determined by replacing a circular opening with an effective rectangular opening having a depth equal to the circular opening diameter  $d_0$  and a width equal to half this diameter [32]. The critical cross-section for determining the Vierendeel bending resistance is then above the upper vertex of the effective rectangular opening. The limiting vertical shear force under VM can therefore be obtained by dividing the plastic capacity of the T-section cross-section by the lever arm equal to half the effective width of the equivalent rectangular opening, formula (1).

$$\frac{V_v}{2} = \frac{M_{pl}}{0.5 \left( \frac{d_0}{2} \right)} \quad (1)$$

If the WPB exhausts the beam load-bearing capacity, then the maximum vertical shear force can be determined using one of the following analytical methods.

### Lawson method - SCI P355

Lawson et al. [15, 30] developed algorithms for determining WPB resistance of composite and non-composite beams for various perforation shapes in the web. The calculation model was created based on the observation of stress distribution between the openings. Bending near the upper and lower opening parts and the action of horizontal shear in the mid-depth of the post generate compressive and tensile forces that act at the opposite diagonals of the post. The trajectories

of these forces intersect at the mid-depth of the post between the openings. The highest normal stresses occur at the edge of the opening, in the plane, for angle  $\theta$  from  $25^\circ$  to  $40^\circ$  relative to the opening axis [30]. On this basis, Lawson et al. [15, 30] proposed a method for predicting web-post buckling capacity by introducing the so-called “strut model”. The model involves determining maximum compression stresses acting on an equivalent strut. Its stability is checked assuming buckling curve c according to EC3 [7] in the same way as in the theory of compression members. The value of the maximum principal stress in the effective strut can be determined from the equilibrium equations with respect to point A (Fig. 3), assuming zero shear stresses around the opening. However, calibrating the stress in the equivalent strut is complicated due to a complex stress state varying around the opening. Therefore, for closely spaced circular openings, Lawson et al. [30] proposed that the value of horizontal shear stresses in the web post should be used for calculation purposes. Stress variability dependent on the depth of the openings and the post’s width is then taken into account by calibrating the effective length of the strut dependent on the same parameters. In the case of circular openings, an assumption is made of the effective restraint point before buckling at the mid-depth of the post; therefore, the effective length of the compression field is half the diagonal length of the post, formula (2).

$$l_{eff, Lawson} = 0.5 \sqrt{s_0^2 + d_0^2} \leq 0.7d_0 \quad (2)$$

The SCI P355 publication [15] updates the previous approach presented by Ward in the SCI P100 publication [29]. The Lawson method is also intended for openings located asymmetricaly at a depth of the web. Then, when determining the stresses acting on the web post, an additional

bending moment in the plane of the post, resulting from the asymmetry of the cross-section, should be taken into account. In this article, formulas are presented only for the symmetrical web perforation situations, which means that the vertical shear force in the upper and lower tee is identical, and no additional bending moment occurs. Normal stresses in the equivalent strut are described by formula (3).

$$\sigma_{Lawson} = \tau_h = \frac{V_h}{s_0 t_w} = \frac{V_v \cdot \frac{s}{h_{eff}}}{s_0 t_w} \quad (3)$$

In order to compare this method with other methods discussed in this article, the Lawson formula [15] was transformed using the relationship between the horizontal and vertical forces. Force  $V_v$  is the design value of the total vertical force acting on the section of the cellular beam along the vertical axis of the web post. The resistance for the maximum vertical shear force is described by formula (4).

$$V_{v,Rd,Lawson} = \chi \frac{s_0 t_w \left(\frac{h_{eff}}{s}\right) f_y}{\gamma_{M1}} \quad (4)$$

$$\begin{aligned} h_{eff} &= H - 2z_t = \\ &= H - 2 \cdot \frac{b_f t_f^2 + t_w s_t^2 - t_w t_f^2}{2(b_f t_f + t_w s_t - t_w t_f)} \end{aligned} \quad (5)$$

The buckling coefficient  $\chi$  is determined based on the relative slenderness in flexural buckling, formula (6), according to the buckling theory of members in compression in PN-EN 1993-1-1 §6.3.1.2. (6.49) [7] with the buckling curve c.

$$\begin{aligned} \bar{\lambda} &= \frac{\lambda}{\lambda_1} = \frac{l_{eff}}{i} \cdot \frac{1}{\lambda_1} = \\ &= \frac{0.5 \sqrt{s_0^2 + d_0^2}}{\frac{t_w}{\sqrt{12}}} \cdot \frac{1}{93.9 \sqrt{\frac{235}{f_y}}} \end{aligned} \quad (6)$$

The method proposed by Lawson et al. [15, 30], also called the SCI P355 method, is calibrated for cellular beams for which the condition  $d_0 \geq s_0 \geq 0.3d_0$  is met, while the assumptions and formulas presented above refer to the situation of closely spaced openings, where  $0.5d_0 > s_0$ .

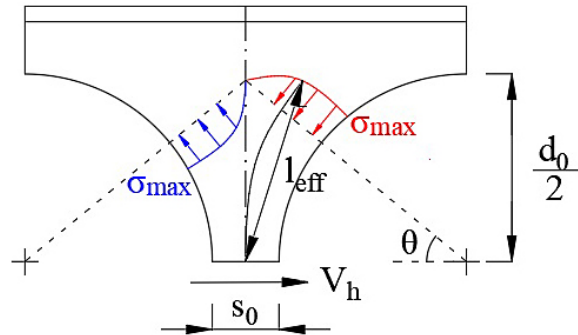


Fig. 3. Strut model by Lawson [30]

### Effective stress modification by Tsavdaridis

Tsavdaridis and D’Mello [32] presented an experimental and numerical study of the failure mode of beams with circular openings and those with a particular shape. They performed 220 complete parametric analyses of elastic-plastic elements to propose an empirical method for evaluating the compressive strength of the web post. Investigations included the effect of the opening diameter-web thickness ratio on the web post stability and the opening spacing-opening diameter ratio on sustaining the effective compression strut for different opening geometries.

The publications of Tsavdaridis and D’Mello [32] and Tsavdaridis and Galiatsatos [33] allow establishing basic assumptions for the calculation model of closely spaced circular openings. The method is very similar to SCI P355 [15]. However, it differs in adopting the effective strut boundary conditions and determining the stresses acting on the strut. Additionally, an assumption was made of the effective width of the compression strut, according to formula (7). The model also assumes that the equivalent compression diagonal strut acts diagonally in the post in its diagonal direction. The authors concluded that the compressive stresses in the diagonal are generated by half of the total vertical shear force, i.e., shear force in the upper tee (formula 8). The strut acts as a bar under compression along the total diagonal length of the post, but the ends of which are modelled as fixed-fixed, therefore due to the assumed boundary conditions, the reduction factor of the effective length is 0.5 (Fig. 4). As a result, the effective length for the unstiffened post is as in formula (2) in Lawson’s method. When a vertical stiffener is used in the post, the reduction factor takes other values, mentioned in the publication by Tsavdaridis and Galiatsatos [33]. Factor

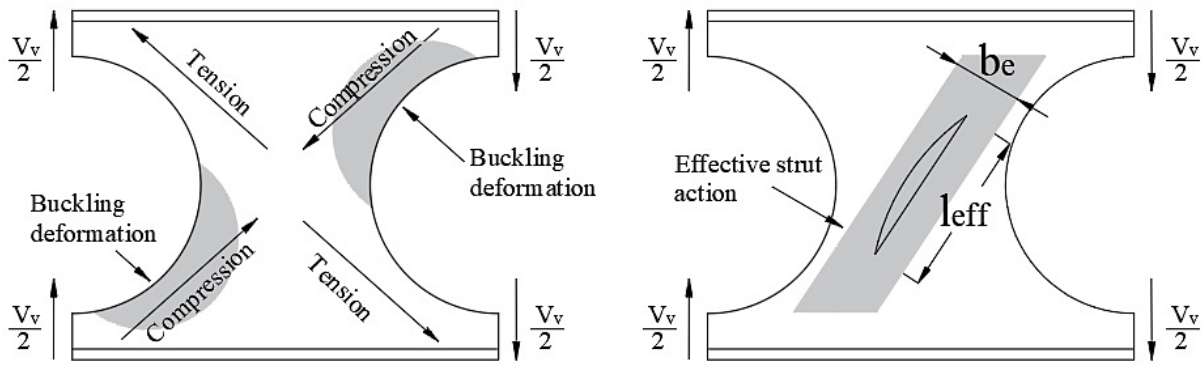


Fig. 4. Forces in web-post and design model according to Tsavdaridis and D’Mello [32]

$\chi$  is to be determined on the basis of the relative slenderness, formula (6), calculated using the effective length of the strut and the buckling curve  $c$ , according to PN-EN 1993-1-1 §6.3.1.2. (6.49) [7]. The total vertical shear resistance in the vertical axis of the post is described by formula (9).

$$b_e = \frac{s_0}{2} \quad (7)$$

$$\sigma_{Tsavdaridis} = \frac{\frac{V_v}{2}}{b_e \cdot t_w} = \frac{V_v}{2 \cdot b_e \cdot t_w} = \frac{V_v}{s_0 t_w} \quad (8)$$

$$V_{v,Rd,Tsavdaridis} = \chi \frac{s_0 t_w f_y}{\gamma_{M1}} \quad (9)$$

### Modification of effective length by Panedpojaman

Unlike in the approach presented by Lawson [15] and Tsavdaridis [32, 33], Panedpojaman et al. [23] defined the length of the strut as equal to half of the segment of the tangent to the adjacent openings, running across the post. The tangent line was used because the stress concentration points occur at the opening edges close to the point of tangency. Adopting half of the tangent length agrees with the assumed location of the stabilisation point in the mid-length of the tangent, as in the Lawson model [15, 30], formula (11). The value of an effective length needs to be determined using a correction factor, formulas (12) and (13). This approach allows including both the elastic restraint due to stress variation in the web post and the size of the area above the opening, which also limits buckling. The value of the correction factor  $k$  depends on the coefficient  $d_0/d$  and spacing ratio  $s/d_0$ , where  $d$  is the initial height of the base section (before the cut). The modification introduces better matching the

strut effective length to different web post widths. The strut from formula (11) is shorter for ratio  $s/d_0 < 1.5$  and longer for  $s/d_0 > 1.5$ , relative to the Lawson effective length from formula (10). A shorter strut increases the buckling strength and, as a result, partially reduces the conservative results obtained from the Lawson model [15, 30] for slender web posts.

$$l_{eff, Lawson} = 0.5 \sqrt{s_0^2 + d_0^2} \quad (10)$$

$$l_{Panedpojaman} = 0.5 \sqrt{s^2 - d_0^2} \quad (11)$$

$$l_{eff, PPM} = k \cdot l_{Panedpojaman} \quad (12)$$

$$k = 0.90 \frac{s}{d_0} \left( \frac{d_0}{d} \right)^2 \leq \min \left( 1.15 \frac{d_0}{d}, 1.15 \right) \quad (13)$$

Compression stress and strength should be determined analogous to the Tsavdaridis method [32], formulas (8) and (9), using the modified effective length of the strut from formula (12) to calculating

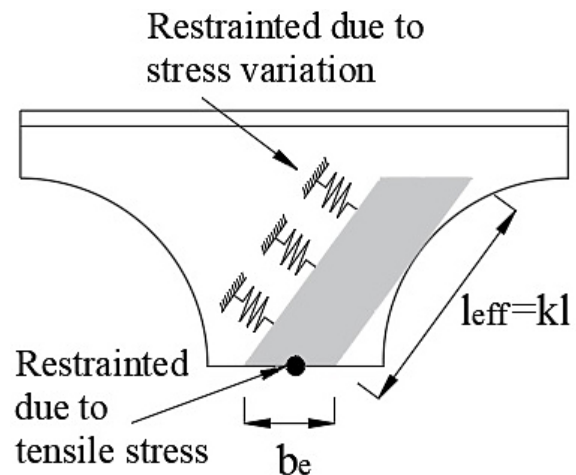


Fig. 5. Design model by Panedpojaman et al. [23]

relative slenderness according to formula (6). Factor  $\chi$  is to be determined according to PN-EN 1993-1-1 §6.3.1.2. (6.49) [7] for buckling curve c.

### Modification of effective length by Wang

Wang et al. [34] investigated the accuracy of determining the compressive stresses in the post according to the methods of Lawson [30], Tsavdaridis [32] and Bitar [31] with the FEM approach. They aimed to make one of the methods applicable for assessing the web post stability in fire conditions. Choosing the Tsavdaridis method [32] for further modifications, they showed that his assumption of an effective width equal to half the post's width at its narrowest point is valid for greater web thicknesses or distances between the edges of adjacent openings. However, it does not work for narrow posts, underestimating the buckling resistance at ambient temperature and during the fire. For thin webs and narrow posts, the effective width  $b_e$  is nearly equal to the post width  $s_0$ . Wang et al. [34] proposed a modification of the effective width of the strut based on the measurements of the bandwidth of compressive stresses in the FEM model. The width depends on the parameters  $s_0$ ,  $d_0$  and  $t_w$ . It can be determined from the following formulas:

$$b_{e,m} = \kappa \cdot \frac{s_0}{2} \tag{14}$$

$$\kappa = a_0 + a_1 \cdot \frac{d_0}{t_w} \tag{15}$$

$$a_0 = b_0 + b_1 \cdot \frac{s}{d_0} \tag{16}$$

$$a_1 = c_0 + c_1 \cdot \frac{s}{d_0} + c_2 \left(\frac{s}{d_0}\right)^2 \tag{17}$$

The fit coefficients for equations (15), (16) and (17) were determined on the basis of the FEM analysis results curve fit and are presented in Table 1. Compression stress and load capacity should be determined analogous to the Tsavdaridis method [32], using the modified effective width of the strut  $b_{em}$ , formula (19). Factor  $\chi$  is to be determined according to PN-EN 1993-1-1 §6.3.1.2. (6.49) [7] for buckling curve c. The relative slenderness is determined according to formula (6) using the effective length according to formula (2).

**Table 1.** Fit coefficients [34]

$b_0 = 0.623962$	$b_1 = 0.487153$	-
$c_0 = 0.072041$	$c_1 = -0.07283$	$c_2 = 0.016533$

$$\sigma_{Wang} = \frac{\frac{V_v}{2}}{b_{e,m} \cdot t_w} = \frac{V_v}{2 \cdot b_{e,m} \cdot t_w} \tag{18}$$

$$V_{v,Rd,Wang} = \chi \frac{2 \cdot b_{e,m} t_w f_y}{\gamma_{M1}} \tag{19}$$

### Bitar Method

CTICM developed the method (Bitar et al. [31]) on behalf of ArcelorMittal as part of the preparatory work for the ACB software development. The method is based on finding the horizontal critical cross-section of a post in which there is a stress concentration from the horizontal shear force acting in the plane of the web. First, the distance of this cross-section from the post's horizontal axis is determined, then the width of the critical cross-section, and finally, its strength is calculated. However, the method has not been fully explained as some details are confidential. Wang et al. [34] compared various methods of determining the compressive stresses in the post with the FEM analysis, using a modified version of Bitar's analytical model for fire conditions. They found that the stresses obtained with this model are extremely high. Therefore, the method of Bitar et al. [31] will not be analysed further in this article.

### Grilo Method

The studies of Grilo et al. [35] confirm the stabilizing role of tensile stresses and the phenomenon of S-shaped buckling. During the loss of stability of a post by buckling, due to the impact of compressive stresses caused by shear force, the post twists around its vertical axis. Grilo et al. [35] proposed a new calculation procedure, verified on the basis of 2545 numerical models and calibrated by laboratory tests of 14 full-size cellular beams. The procedure is similar to the assumptions of Bitar et al. [31]. However, in this case, the algorithm is more extensive and allows taking the complex state of stresses around the openings into account. The laboratory tests were performed on simply supported beams with four circular openings, loaded in the mid-span with a concentrated force acting on the central post with

stiffeners. Since the support post is also stiffened, WPB occurs only in two unstiffened posts. For particularly slender posts, the so-called border effect can occur that consists of WPB followed by a further load increase due to the post-critical Vierendeel mechanism acting on the frame surrounding the two openings made of T-sections and stiffened posts (Fig. 6.). Grilo et al. [35] eliminated the border effect by conducting numerical analyses on long beam models with more openings and posts. Based on these observations, they calibrated a new single web post model that is insensitive to the border effect. The WPB phenomenon for closely spaced openings is mainly due to the action of horizontal shear, as also stated by Lawson [15, 30], so the single web post model was considered adequate for calibrating the empirical analytical procedure.

The horizontal shear force  $V_h$  causes bending with increasing distance from the horizontal axis of the web post. An internal bending moment develops and increases towards the T-section. However, as the cross-section of the web post widens in the direction of the increasing bending moment, the bending stresses increase up to a maximum value at a certain critical distance and then decrease, spreading over a larger area. After determining the arm for the critical cross-section, the critical cross-section area should be established, where yielding occurs due to interacting normal and shear stresses, formulas (20) and (21). This phenomenon is non-linear and the yield line is not necessarily straight; therefore, the analytical model is calibrated using additional coefficients while accepting some approximations. To include the complex stress state, Grilo et al. [35] introduced the equivalent yield strength to determine the maximum normal stresses and the equivalent shear strength to determine the maximum shear stresses. The value of the equivalent yield point

matches the maximum stress induced by bending with horizontal shear force  $V_h$  on the arm  $y$  with the cross section defined by the plastic modulus. The equivalent shear strength corresponds to the maximum shear force that can be contained by the transverse cross section of the web post. The interaction of normal and shear stresses is determined by a mutual relationship between the equivalent yield strength and equivalent shear strength with respect to the first yield strength  $f_y$  of the material based on the von Mises reduced stresses criterion (H-M-H hypothesis). By isolating the value of the horizontal shear force  $V_h$  from this relationship, the horizontal plastic shear resistance can be determined. The horizontal shear value  $V_h$  from this relationship allows determining the horizontal plastic shear capacity. This value is calibrated using both the approximated empirical formula for  $y_{pl}$  and empirical efficiency factor  $\mu$  (1.00 do 1.23) according to formulas (23) and (25). Plastic resistance for the vertical shear force  $V_v$  can be obtained using the interdependence between the horizontal and vertical forces determined from the equilibrium equations, using the  $h_{eff}$  distance determined from (5). The value of the design vertical shear resistance due to buckling of the web post, formula (28), is determined using the buckling coefficient  $\chi$ , which reduces the plastic shear resistance of the cross-section, and the partial material factor to determine the resistance with consideration of element stability [7]. Factor  $\chi$  is calculated using empirical formulas (26) and (27) for two situations dependent on the size of the dimensionless relative slenderness from (25). The factor values for formulas (26) and (27) are presented in Table 2.

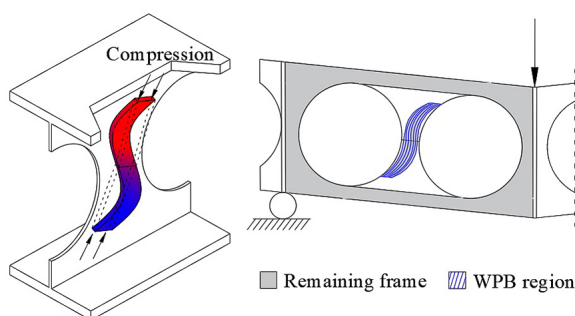


Fig. 6. Web post instability due to buckling and post-critical Vierendeel bending mechanism by Grilo et al. [35]

$$y_{pl} = \frac{d_0}{2} \left[ 0.445 \left( \frac{s}{d_0} \right)^3 - 2.578 \left( \frac{s}{d_0} \right)^2 + 4.770 \left( \frac{s}{d_0} \right) - 2.475 \right] \quad (20)$$

$$b_{pl} = s - d_0 \sqrt{1 - \frac{4y_{pl}^2}{d_0^2}} \quad (21)$$

$$V_{h,Rk} = V_{h,pl} \cdot \chi = \mu \cdot f_y \frac{t_w b_{pl}^2}{\sqrt{3b_{pl}^2 + 16y_{pl}^2}} \cdot \chi \quad (22)$$

$$\mu = 1.198 - 0.42 \frac{d_0}{H} + \frac{s}{5d_0} \text{ for } \frac{s}{d_0} < 1.2 \quad (23)$$

**Table 2.** Values of coefficients for determining buckling coefficient  $\chi$  [35]

$d_0/H$	$s/d_0$	Coefficient					$d_0/H$	$s/d_0$	Coefficient				
		$\alpha$	$\beta$	$\gamma$	$\epsilon$	$\eta$			$\alpha$	$\beta$	$\gamma$	$\epsilon$	$\eta$
0.5	1.1	0.759	1.35	1.15	0.660	3.5	0.7	1.1	0.849	1.47	1.08	0.786	4.5
	1.2	0.730	1.39	1.42	0.514	2.1		1.2	0.844	1.44	1.11	0.760	3.9
	1.3	0.780	1.40	1.16	0.672	3.5		1.3	0.903	1.39	1.15	0.785	4.0
	1.4	0.840	1.42	1.26	0.667	2.7		1.4	0.980	1.34	1.12	0.870	3.0
	1.5	0.916	1.40	1.09	0.840	5.0		1.5	1.130	1.33	-	-	-
0.6	1.1	0.798	1.42	1.14	0.700	3.5	0.8	1.1	0.888	1.46	1.09	0.815	4.0
	1.2	0.791	1.42	1.13	0.700	3.8		1.2	0.901	1.42	1.14	0.790	3.5
	1.3	0.836	1.40	1.10	0.760	4.5		1.3	1.020	1.42	-	-	-
	1.4	0.909	1.36	1.15	0.790	3.3		1.4	1.175	1.42	-	-	-
	1.5	0.970	1.31	1.09	0.890	4.5		1.5	1.285	1.36	-	-	-

$$\mu = 1.838 - 0.42 \frac{d_0}{H} - \frac{s}{3d_0} \text{ for } \frac{s}{d_0} \geq 1.2 \quad (24)$$

$$\bar{\lambda} = \frac{\lambda}{\pi} \sqrt{\frac{f_y}{E}} = \sqrt{\frac{3(s^2 - d_0^2)f_y}{\pi^2 t_w^2 E}} \quad (25)$$

$$\chi = \frac{\alpha}{\bar{\lambda}^\beta} \leq 1.0 \text{ for } \bar{\lambda} \geq 1.0 \quad (26)$$

$$\chi = \gamma \cdot \epsilon^{(\bar{\lambda}^\eta)} \leq 1.0 \text{ for } \bar{\lambda} < 1.0 \quad (27)$$

$$V_{v,Rd,Grilo} = \frac{V_{h,Rk} \left( \frac{h_{eff}}{s} \right)}{\gamma_{M1}} \quad (28)$$

## COMPARISON OF METHODS

### Initial assumptions

The methods and their modifications were compared using seven beam geometries for which WPB failure was demonstrated experimentally and numerically in the literature [23, 35]. Beam B1-B3

were made of the American W310x21.0 (W12x14) profiles, beam B4 was made of the W310x28.3 (W12x19) profile, according to [35]. Beams B5 and B6 were fabricated from the European IPE400 profiles, and beam B7 was manufactured from the HEB400 profile, according to [23]. Average geometric dimensions measured after fabrication were adopted for the analysis except for the initial section depth  $d$  (before cutting). For the initial section depth  $d$ , used to determine the correction factor  $k$  in the modification of Panedpojaman et al. [23], standard denominations were used. For all analysed beams, the nominal yield strength  $f_y$  for steel S235 was adopted; therefore, the material properties did not affect the assessment of the methods described. Data for analytical calculations are included in Table 3. In the method of Grilo et al. [35], the coefficients  $\alpha, \beta, \gamma, \epsilon, \eta$  for the intermediate  $d_0/H$  and  $s/d_0$  ratios in the analysed beams were determined based on the linear interpolation.

Parameter  $V_{v,Rd}$  to be determined is the buckling load capacity of the web post, which should be compared with the total vertical shear force  $V_{v,Ed}$  acting on the beam cross-section in the vertical axis of the web post.

**Table 3.** Geometric quantities for analytical calculations

Name	$b_f$ [mm]	$t_f$ [mm]	$t_w$ [mm]	$d_0$ [mm]	H [mm]	s [mm]	$s_0$ [mm]	$f_y$ [MPa]	d [mm]	$d_0/t_w$	$d_0/H$	$s/d_0$	$d_0/d$	$s_f$ [mm]	$Z_t$ [mm]
B1	102	5.6	4.8	342.5	433.0	445.8	103.3	235	302	71.35	0.79	1.30	1.13	45.3	8.466068
B2	104	6.2	4.7	343.9	433.0	483.2	139.3	235	302	73.17	0.79	1.41	1.14	44.6	7.976774
B3	103	5.8	4.9	250.0	407.0	350.1	100.1	235	302	51.02	0.61	1.40	0.83	78.5	17.561900
B4	98	9.2	6.0	245.0	409.0	343.0	98.0	235	309	40.83	0.60	1.40	0.79	82.0	17.980753
B5	180	13.5	8.6	358.0	558.0	480.0	122.0	235	400	41.63	0.64	1.34	0.90	100.0	18.469021
B6	180	13.5	8.6	430.0	600.0	485.0	55.0	235	400	50.00	0.72	1.13	1.08	85.0	15.332630
B7	300	24.0	13.5	422.0	599.0	485.0	63.0	235	400	31.26	0.70	1.15	1.06	88.5	16.774115

**RESULTS**

The calculations were performed using the MS Excel spreadsheet. The empirical correction factors and buckling parameters were rounded to the sixth decimal place. Results for the methods based on the compression strut

model are presented in Tables 5-11 and the final formulas used for the analytical calculations are shown in Table 4. Analytically calculated load capacity for each of the beams are presented in Figure 7, distinguishing between the individual methods described in this article [15, 30, 32, 33, 23, 34, 35].

**Table 4.** Final formulas for analytical calculations

Method	Effective length [mm]	Relative slenderness [-]	Buckling coefficient $\chi$ [-]	Effective width [mm]	$\sigma$ for $V_v=1\text{kN}$ [MPa]	$V_{v,Rd}$ [kN]
Lawson	Eq. (2)	Eq. (6)	PN-EN 1993-1-1 § 6.3.1.2. Eq. (6.49) for $\alpha=0.49$	N/A	Eq. (3)	Eq. (4)
Tsavdaridis				Eq. (7)	Eq. (8)	Eq. (9)
Panedpojaman	Eq. (12)	Eq. (6)				Eq. (9)
Wang	Eq. (2)	Eq. (6)		Eq. (14)	Eq. (18)	Eq. (19)
Grilo	-					Eq. (28)

**Table 5.** Results for B1

Method	Effective length [mm]	Relative slenderness [-]	Buckling coefficient $\chi$ [-]	Effective width [mm]	$\sigma$ for $V_v=1\text{kN}$ [MPa]	$V_{v,Rd}$ [kN]
Lawson	178.8695	1.3704	0.3604	N/A	2.161	39.194
Tsavdaridis				51.65	2.017	41.995
Panedpojaman	164.0831 (-8.3%)	1.2571 (-8.3%)	0.4074 (+13.0%)			47.471
Wang	178.8695	1.3704	0.3604	84.3449 (+63.3%)	1.235	68.578
Grilo	-					48.822

**Table 6.** Results for B2

Method	Effective length [mm]	Relative slenderness [-]	Buckling coefficient $\chi$ [-]	Effective width [mm]	$\sigma$ for $V_v=1\text{kN}$ [MPa]	$V_{v,Rd}$ [kN]
Lawson	185.5207	1.4527	0.3304	N/A	1.770	43.874
Tsavdaridis				69.65	1.527	50.834
Panedpojaman	195.1742 (+5.2%)	1.5283 (+5.2%)	0.3055 (-7.5%)			47.003
Wang	185.5207	1.4527	0.3304	103.1092 (+48.0%)	1.032	75.255
Grilo	-					54.335

**Table 7.** Results for B3

Method	Effective length [mm]	Relative slenderness [-]	Buckling coefficient $\chi$ [-]	Effective width [mm]	$\sigma$ for $V_v=1\text{kN}$ [MPa]	$V_{v,Rd}$ [kN]
Lawson	134.6477	1.0170	0.5301	N/A	1.919	64.903
Tsavdaridis				50.05	2.039	61.102
Panedpojaman	105.8429 (-21.4%)	0.7994 (-21.4%)	0.6625 (+25.0%)			76.363
Wang	134.6477	1.0170	0.5301	71.6888 (+43.2%)	1.423	87.519
Grilo	-					65.895

**Table 8.** Results for B4

Method	Effective length [mm]	Relative slenderness [-]	Buckling coefficient $\chi$ [-]	Effective width [mm]	$\sigma$ for $V_v=1\text{kN}$ [MPa]	$V_{v,Rd}$ [kN]
Lawson	131.9365	0.8122	0.6545	N/A	1.564	98.359
Tsavidaridis						90.439
Panedpojaman	95.0718 (-27.9%)	0.5852 (-27.9%)	0.7941 (+21.3%)	49.00	1.701	109.729
Wang	131.9365	0.8122	0.6545	68.9629 (+40.7%)	1.208	127.284
Grilo	-					84.726

**Table 9.** Results for B5

Method	Effective length [mm]	Relative slenderness [-]	Buckling coefficient $\chi$ [-]	Effective width [mm]	$\sigma$ for $V_v=1\text{kN}$ [MPa]	$V_{v,Rd}$ [kN]
Lawson	189.1084	0.8121	0.6546	N/A	0.878	175.206
Tsavidaridis						161.399
Panedpojaman	154.5321 (-18.3%)	0.6636 (-18.3%)	0.7470 (+14.1%)	61.00	0.953	184.182
Wang	189.1084	0.8121	0.6546	88.3490 (+44.8%)	0.658	233.762
Grilo	-					145.261

**Table 10.** Results for B6

Method	Effective length [mm]	Relative slenderness [-]	Buckling coefficient $\chi$ [-]	Effective width [mm]	$\sigma$ for $V_v=1\text{kN}$ [MPa]	$V_{v,Rd}$ [kN]
Lawson	216.7516	0.9308	0.5811	N/A	1.801	75.824
Tsavidaridis						64.592
Panedpojaman	128.9911 (-40.5%)	0.5539 (-40.5%)	0.8124 (+39.8%)	27.50	2.114	90.302
Wang	216.7516	0.9308	0.5811	47.2952 (+72.0%)	1.229	111.087
Grilo	-					51.031

**Table 11.** Results for B7

Method	Effective length [mm]	Relative slenderness [-]	Buckling coefficient $\chi$ [-]	Effective width [mm]	$\sigma$ for $V_v=1\text{kN}$ [MPa]	$V_{v,Rd}$ [kN]
Lawson	213.3383	0.5826	0.7957	N/A	1.008	185.416
Tsavidaridis						159.035
Panedpojaman	137.4491 (-35.6%)	0.3753 (-35.6%)	0.9103 (+14.4%)	31.50	1.176	181.939
Wang	213.3383	0.5826	0.7957	47.3110 (+50.2%)	0.783	238.860
Grilo	-					97.557

## DISCUSSION

Each of the methods discussed above refers to similar observations of the behaviour of the web post under load. Both numerical simulations and

experimental studies confirm the occurrence of the S-shaped web-post buckling due to intersecting trajectories of compressive and tensile stresses. The goal is to determine the stresses acting on the web post and to investigate its stability under

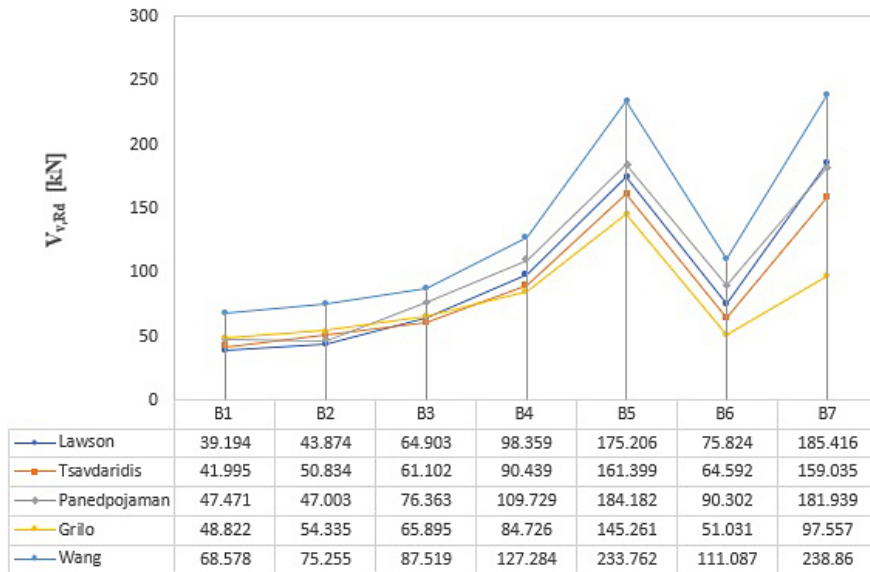


Fig. 7. Vertical shear force resistance for the discussed methods

buckling load following the analogy to compression member buckling as per PN-EN 1993-1-1 [7].

In the method by Lawson et al. [15, 30], which is an update of Ward’s method (SCI P100) [29], the compressive stresses acting on the effective strut are approximated by shear stresses caused by the horizontal shear force at mid-depth of the web post. In order to be able to compare the value of the load capacity calculated from this method with other methods, the interdependence of the horizontal force with the vertical shear force was used. The method of Tsavdaridis et al. [32, 33] analysed in this article differs from the method of Lawson et al. [15, 30] only in that, for simplicity, the compressive stresses in the effective strut are approximated by the vertical shear force in the upper tee, i.e., with half of the total vertical shear force acting on the effective web width. Thus, the difference in the bearing capacity formula is that formula (4) of the Lawson method has an additional coefficient  $h_{eff}/s$ . The Lawson resistance is higher when this factor is greater than 1 when the horizontal shear force is less than the total vertical shear force. This is the case when the  $h_{eff}$  is greater than the opening axial spacing  $s$ , as in beams B3-B7. In beams B1 and B2, Lawson’s resistance is lower than that provided by Tsavdaridis. The ratio of load capacities obtained from these two methods is inversely proportional to the assumed ratio of compressive stresses. The difference between these methods for the analysed beam geometries is from a few to a dozen or so per cent, Table 12. In general, according to SCI P355 [15], the

limits of using the Lawson method with assumptions for closely spaced openings are as follows:  $0.3d_0 \leq s_0 \leq 0.5d_0$ . This condition is not met for beams B6 and B7 because  $s_0 < 0.3d_0$ , i.e.,  $0.13d_0$  and  $0.15d_0$  respectively.

Panedpojaman et al. [23] adopted the assumptions of Tsavdaridis et al. [32, 33] with a modification of the strut length, which for  $s/d_0 < 1.5$  is always shorter. However, in order to obtain the effective length, the  $k$ -factor must additionally be used, taking into account the effect of the size of the area above the openings and the variability of stresses around the openings on the restraint of the strut. For this reason, the resistance according to Panedpojaman [23] is higher than that given by Tsavdaridis, except for the B2 beam, for which a greater value of the effective length was obtained as a result of the modification with the  $k$  factor. Figure 7 shows that Panedpojaman’s load capacity for beams B3 and B4 is higher. At the same time, the Lawson, Tsavdaridis

Table 12. Comparison of load bearing capacities for Lawson and Tsavdaridis methods

Beams	$\alpha = \frac{h_{eff}}{s} = \frac{\sigma_{Tsavdaridis}}{\sigma_{Lawson}} = \frac{V_{v,Rd,Lawson}}{V_{v,Rd,Tsavdaridis}}$
B1	0.933306
B2	0.863093
B3	1.062200
B4	1.087576
B5	1.085546
B6	1.173886
B7	1.165880

and Grilo methods give lower but similar results. This is due to a simultaneous drop of  $d_o/H$  (0.61 and 0.60, respectively) and  $d_o/d$  (0.83 and 0.79) ratios, indicating a large area above the openings. Its beneficial effect is included in the Panedpojaman method via the modification factor  $k$ . The relative slenderness value varies in proportion to the decrease in effective length, Tables 5-11. After Panedpojaman's modification, the effective length of the strut decreased compared with the Tsavdaridis method by an average of 22.5% for beams B3-B5 and 40.5% for beam B6, which resulted in a nearly 40% higher buckling coefficient  $\chi$  for this beam. The higher load capacity from Lawson compared with that of Panedpojaman for beam B7 beam is not taken into account because, as previously stated, beams B6 and B7 did not meet the criteria for SCI P355 [15] application.

The experimental tests of Tsavdaridis and D'Mello [32] were limited to short beams ( $L = 1.7\text{m}$ ) with thin webs, opening diameter  $d_o = 0.7d$ , and the ratio  $s/d_o = 1.3$ . Based on the tests, they calibrated the FE model of a single web post. Panedpojaman [23] investigated experimentally more diverse short and long composite and non-composite beams, while for numerical simulations he also used a single web post model based on the Tsavdaridis and D'Mello model [32]. The assumption that the strut's effective width  $b_e = s_o/2$  is considered a conservative approximation for low  $d_o/d$  and  $s/d_o$  ratios. Panedpojaman et al. [23] admit that their analytical method for thin and narrow posts ( $s/d_o = 1.1$ ) leads to a significant underestimation of the load capacity by 47% on average, while the methods of Tsavdaridis and Lawson give even lower results. As the width of the web post increases, the actual width of the compression field decreases, and for ratios  $s/d_o > 1.5$  it becomes closer to the value  $s_o/2$ . To ensure safe results of the analytical methods, Panedpojaman et al. [23] and Tsavdaridis and D'Mello [32] adopted a constant value of the effective width for all geometries. In this article, beams B5, B6 and B7 correspond to the geometry of beams NB5, NB7 and NB6, respectively, [23], only the value of the yield stress  $f_y$  is different. The analytical results in [23] for these beams are 4%, 18%, and 26% lower than the numerical model of a single web post. Therefore, it can be concluded that for the B6 and B7 beams with narrow posts ( $s/d_o = 1.1$ ), the results obtained were conservative.

The load capacity determined by taking into account the modified effective width according

to Wang et al. [34] is much higher than capacities determined according to other methods. The method is an alternative version of Tsavdaridis and D'Mello's method [32], differing only in adopting a larger effective width. The empirical formulas of Wang et al. [34] are based on numerical simulations based on the Tsavdaridis and D'Mello short beam model [32] with the initial imperfection of the web increased from  $t_w/200$  to 1mm. The model has four openings on the web, and the support posts and the central post are stiffened. During experimental tests of such beams, Grilo et al. [35] found it difficult to determine the critical load due to the strong influence of the border effect that occurs for the adopted laboratory conditions. There is also the fact that the study of Tsavdaridis and D'Mello [32] was quite limited. Therefore, the modification based on the width measurement of the compressive stress band in the web post using such a FEM model is still unreliable. However, considering that the method of Panedpojaman et al. [23] leads to conservative results under certain conditions, the actual load capacity results can be limited by the Panedpojaman method from below and by the Wang method from above, especially for beams B6 and B7, for which  $s/d_o = 1.1$ .

Grilo et al. [35] developed a different analytical procedure but based on similar observations. They tested short beams with thin webs (5.0 mm and 6.0 mm nominal thickness) and noticed the influence of the border effect, especially for the ratios  $s/d_o = 1.15$  and  $d_o/H = 0.8$ , for which large deformations occurred. Similar geometric relationships appeared in the B6 and B7 beams tested in the current article. Numerical analyses allowed Grilo et al. [35] to isolate this effect and develop a new modified FEM model of a single web post. They found that the single web post model of Panedpojaman [23] and Tsavdaridis [32] used unrealistic ideal boundary conditions. For the geometry of the B1, B2, B3 and B4 beams specified in the article by Grilo et al. [35] as beams A2, A3, A6 and B6, the analytical results were verified with numerical results, assuming the measured values of the yield strength according to [35]. It was found that the analytical load capacity is exceptionally close to the numerical results for the single web post model - the maximum difference on the safe side did not exceed 5%, while the analytical load capacity was lower by an average of 14% relative to the experimental tests. From Figure 7, it follows that the analytical load capacity

of the Grilo method is quite similar to the load capacity obtained by Lawson [15], Tsavdaridis and D’Mello [32] and Panedpojaman [23] for beams with thin webs and wider posts - B1, B2, B3 and B4. The method gives lower results for beams with thicker and narrower webs - beams B5, B6 and B7. The most significant deviation occurred for the B7 beam with a narrow post ( $s/d_o = 1.15$ ) and the web much thicker than in the other beams ( $t_w = 13.5$  mm). The lower value of the bearing capacity compared to other methods may be related to the separation of the influence of the border effect for this type of web geometry.

## SUMMARY AND CONCLUSIONS

This study discusses the behaviour of cellular beams under load and names typical modes of failure. Two forms of capacity loss were distinguished in detail, i.e., web-post buckling (WPB) and Vierendeel’s mechanism (VM) in the case of beams secured against lateral torsional buckling. Analytical models for calculating the buckling resistance of the web post for beams with closely spaced circular openings in the web were presented. Care was taken to ensure that the nomenclature of different algorithms was consistent (according to EN 1993-1-1 [7]) and expressed the resistance to vertical shear force. Then, the load capacity calculated according to each analytical method was compared for seven beam geometries for which WPB failure mode was demonstrated in experimental and numerical analyses in the scientific literature [23, 35]. The study aimed to investigate the interrelationships between these methods and discuss the discrepancies between the obtained results.

Each algorithm was implemented in MS Excel, and the results were tabulated in Tables 5-11 and plotted in Figure 7. The differences between the methods are significant, as demonstrated in this study, especially for beams with narrow posts.

The discrepancies result from a relatively small number of experimental studies focused on capturing the WPB phenomenon and the interaction between WPB and VM. Moreover, the tests are usually limited to less geometrically differentiated short-span beams in which shear can cause a border effect. For this reason, the numerical models of different authors vary on some issues, especially when it comes to the single web post model. Such models are used by Tsavdaridis and

D’Mello [32], Panedpojaman et al. [23] and Grilo et al. [35]. While the first two [32, 23] are similar, the model [35] adopts much less optimistic boundary conditions.

Wang et al. [34] used the numerical model of the short beam of Tsavdaridis and D’Mello [32] with slight modifications, on the basis of which they measured the width of the compressive stress band in the web post. The increased effective width leads to a much higher load capacity than in the other methods. However, for narrow posts ( $s/d_o = 1.1$ ), the Lawson, Tsavdaridis and Panedpojaman methods are considered conservative even by the authors themselves. The different method by Grilo et al. [35] is quite convergent with the other methods for wider web posts but for thicker and narrow posts, it provides much lower results, Figure 7. This may be due to border effect elimination and adoption of more conservative boundary conditions in the numerical model. However, Grilo’s analytical procedure shows very good agreement with his numerical model. It is thus necessary to verify the assumptions of the numerical models used by the authors mentioned above.

Further testing of widely varying beams is therefore needed to eliminate the error in the methods for extreme relationships between  $s/d_o$ ,  $d_o/H$ ,  $d_o/d$  and  $d_o/t_w$  ratios. A detailed study of FEM models is needed in order to establish appropriate boundary conditions and analysis parameters for a single web post model. Finally, it is necessary to verify the correctness and identify inconsistencies in the numerical models used to calibrate analytical methods [32, 23, 35, 34] to assess the individual methods unequivocally. This paper attempts to demonstrate the points of issue in different computational methods. The discussion enabled outlining directions for further work aiming at verification of assumptions of numerical models and establishment of reliable guidelines for designers. Determining accurate design procedure will contribute to the optimal design of openwork structures while maintaining an adequate level of safety.

## REFERENCES

1. Espion B. The Vierendeel bridge at its heyday: Rational design, experiments and brittle failure. *Nuts & bolts of construction history*. 2012; 3: 253–260.
2. Łubiński M., Filipowicz A., Żółtowski W. *Metal Structures. Part 1*. Arkady; Warsaw, 2000. (in Polish)

3. Tsavdaridis K.D., Kingman J.J., Toropov V.V. Application of structural topology optimisation to perforated steel beams. *Computers and Structures*. 2015; 158: 108–123.
4. ArcelorMittal. ACB® and Angelina® beams. A new generation of beams with large web openings. ArcelorMittal; Luxembourg, 2021. Available in: [https://sections.arcelormittal.com/repository2/Sections/5\\_4\\_1\\_Beams%20with%20large%20web%20openings.pdf](https://sections.arcelormittal.com/repository2/Sections/5_4_1_Beams%20with%20large%20web%20openings.pdf)
5. Sonck D., Van Impe R., Belis J. Experimental investigation of residual stresses in steel cellular and castellated members. *Construction and Building Materials*. 2014; 54: 512–519.
6. Sonck D., Belis J. Lateral-torsional buckling resistance of cellular beams. *J. Construct. Steel Research*. 2015; 105: 119–128.
7. PN-EN 1993-1-1:2006, Eurocode 3: Design of steel structures – Part 1-1: General rules and rules for buildings. Polish Committee for Standardization; Warsaw, June 2006 ed. (in Polish)
8. Bródka J., Broniewicz M. Design of steel structures according to Eurocodes. Engineer's handbook. PWT; Rzeszów, 2013. (in Polish)
9. Erdal F., Saka M.P. Ultimate load carrying capacity of optimally designed steel cellular beams. *J. Construct. Steel Research*. 2013; 80: 355–368.
10. Najafi M., Wang Y.C. Behaviour and design of steel members with web openings under combined bending, shear and compression. *J. Construct. Steel Research*. 2017; 128: 579–600.
11. El-Sawy K.M., Sweedan A.M.I., Martini M.I. Moment gradient factor of cellular steel beams under inelastic flexure. *J. Construct. Steel Research*. 2014; 98: 20–34.
12. Ellobody E. Nonlinear analysis of cellular steel beams under combined buckling modes. *Thin-Walled Structures*. 2012; 52: 66–79.
13. Panedpojaman P., Sae-Long W., Chub-Uppakarn T. Cellular beam design for resistance to inelastic lateral-torsional buckling. *Thin-Walled Structures*. 2016; 99: 182–194.
14. Fares S.S., Coulson J., Dinehart D.W. AISC design guide 31: castellated and cellular beam design. American Institute of Steel Construction. Chicago, 2016.
15. Lawson R.M., Hicks S.J. Design of composite beams with large web openings: in accordance with Eurocodes and the UK National Annexes. Steel Construction Institute. 2011; SCI P355.
16. Chung K.F., Liu T.C.H., Ko A.C.H. Investigation on Vierendeel mechanism in steel beams with circular web openings. *J. Construct. Steel Research*. 2001; 57: 467–490.
17. Chung K.F., Liu C.H., Ko A.C.H. Steel beams with large web openings of various shapes and sizes: an empirical design method using a generalised moment-shear interaction curve. *J. Construct. Steel Research*. 2003; 59: 1177–1200.
18. Tsavdaridis K.D., D'Mello C. Vierendeel bending study of perforated steel beams with various novel web opening shapes, through non-linear finite element analyses. *Journal of Structural Engineering*. 2012; 138(10): 1214–1230.
19. Panedpojaman P., Thepchatri T., Limkatanyu S. Novel simplified equations for Vierendeel design of beams with (elongated) circular openings. *J. Construct. Steel Research*. 2015; 112: 10–21.
20. Kalkan I., Buyukkaragoz A. A numerical and analytical study on distortional buckling of doubly-symmetric steel I-beams. *J. Construct. Steel Research*. 2012; 70: 289–297.
21. AISI S100-16w/S1-18. North American Specification for the design of cold-formed steel structural members. American Iron and Steel Institute; Washington, DC, USA 2018.
22. BS 5950-1:2000. Structural use of steelwork in building. Part 1: Code of practice for design – Rolled and welded sections. British Standards Institution; 2001.
23. Panedpojaman P., Thepchatri T., Limkatanyu S. Novel design equations for shear strength of local web-post buckling in cellular beams. *Thin-Walled Structures*. 2014; 76: 92–104.
24. Hoffman R., Dinehart D., Gross S., Yost J. Analysis of stress distribution and failure behavior of cellular beams. In: Proc. of International Ansys Conference, Pittsburgh, PA, USA 2006. Available in: [https://www.academia.edu/19205824/Analysis\\_of\\_Stress\\_Distribution\\_and\\_Failure\\_Behavior\\_of\\_Cellular\\_Beams](https://www.academia.edu/19205824/Analysis_of_Stress_Distribution_and_Failure_Behavior_of_Cellular_Beams)
25. Łysa M., Ruchwa M. Nonlinear static analysis of perforated beams with cellular openings. In: Kiczowski T. (ed.) Polyoptimization and computer-aided design. Koszalin University of Technology. 2014; 12: 145–161. (in Polish)
26. Jamadar A.M., Kumbhar P.D. Finite element analysis of castellated beam: A review. *International J. of Innovative Research in Advanced Engineering*. 2014; 1(9): 125–129.
27. De Oliveira J.P. Design equations for local buckling of castellated beams subjected to pure bending [Ph.D. Thesis]. Pontificia Universidade Católica do Rio de Janeiro. 2017. Available in: <https://www.maxwell.vrac.puc-rio.br/36634/36634.PDF>
28. Tsavdaridis K.D. Structural performance of perforated steel beams with novel web openings and with partial concrete encasement [Unpublished Doctoral Thesis]. City University London. 2010. Available in: <https://openaccess.city.ac.uk/id/eprint/11660>
29. Ward J.K. Design of composite and non-composite cellular beams. Steel Construction Institute. 1990; SCI P100.

30. Lawson R.M., Lim J., Hicks S.J., Simms W.I. Design of composite asymmetric cellular beams and beams with large web openings. *J. Construct. Steel Research*. 2006; 62: 614–629.
31. Bitar D., Demarco T., Martin P.O. Steel and composite cellular beams – Novel approach for design based on experimental studies and numerical investigations. In: *Proc. of the 4th European Conference on Steel and Composite Structures – EUROSTEEL 2005*, Maastricht, The Netherlands 2005; Volume B:1.10-1–1.10-8.
32. Tsavdaridis K.D., D’Mello C. Web buckling study of the behaviour and strength of perforated steel beams with different novel web opening shapes. *J. Construct. Steel Research*. 2011; 67: 1605–1620.
33. Tsavdaridis D.K., Galiatsatos G. Assessment of cellular beams with transverse stiffeners and closely spaced web openings. *Thin-Walled Structures*. 2015; 94: 636–650.
34. Wang P., Wang X., Liu M. Practical method for calculating the buckling temperature of the web-post in a cellular steel beam in fire. *Thin-Walled Structures*. 2014; 85: 441–455.
35. Grilo L.F., Fakury R.H., de Castro e Silva A.L.R., de Souza Verissimo G. Design procedure for web-post buckling of steel cellular beams. *J. Construct. Steel Research*. 2018; 148: 525–541.
36. Zaher O.F., Yossef N.M., El-Boghdadi M.H., Dabaon M.A. Structural behaviour of arched steel beams with cellular openings. *J. Construct. Steel Research*. 2018; 148: 756–767.
37. Ferreira F.P.V., Martins C.H., De Nardin S. Assessment of web post buckling resistance in steel-concrete composite cellular beams. *Thin-Walled Structures*. 2021; 159: 106969.
38. Kang L., Hong S., Liu X. Shear behaviour and strength design of cellular beams with circular or elongated openings. *Thin-Walled Structures*. 2021; 160: 107353.
39. Justino L.G., Ribeiro J.C.L., de Souza Verissimo G., Paes J.L.R., Pedroti L.G. Shear buckling strength of web-posts in castellated beams in fire. *Engineering Structures*. 2020; 209: 109960.